THE ANATOMICAL RECORD 296:670–680 (2013)

Trigeminal Nerve Morphology in *Alligator mississippiensis* and Its Significance for Crocodyliform Facial Sensation and Evolution

IAN D. GEORGE AND CASEY M. HOLLIDAY*
Integrative Anatomy, Department of Pathology and Anatomical Sciences, University of Missouri, Columbia, Missouri, USA

ABSTRACT

Modern crocodylians possess a derived sense of face touch, in which numerous trigeminal nerve-innervated dome pressure receptors speckle the face and mandible and sense mechanical stimuli. However, the morphological features of this system are not well known, and it remains unclear how the trigeminal system changes during ontogeny and how it scales with other cranial structures. Finally, when this system evolved within crocodyliforms remains a mystery. Thus, new morphological insights into the trigeminal system of extant crocodylians may offer new paleontological tools to investigate this evolutionary transformation. A cross-sectional study integrating histological, morphometric, and 3D imaging analyses was conducted to identify patterns in cranial nervous and bony structures of *Alligator mississippiensis*. Nine individuals from a broad size range were CT-scanned followed by histomorphometric sampling of mandibular and maxillary nerve divisions of the trigeminal nerve. Endocast volume, trigeminal fossa volume, and maxillomandibular foramen size were compared with axon counts from proximal and distal regions of the trigeminal nerves to identify scaling properties of the structures. The trigeminal fossa has a significant positive correlation with skull length and endocast volume. We also found that axon density is greater in smaller alligators and total axon count has a significant negative correlation with skull size. Six additional extant and fossil crocodyliforms were included in a supplementary scaling analysis, which found that size was not an accurate predictor of trigeminal anatomy. This suggests that phylogeny or somatosensory adaptations may be responsible for the variation in trigeminal ganglion and nerve size in crocodyliforms. Anat Rec, 296:670–680, 2013. © 2013 Wiley Periodicals, Inc.

Key words: alligator; crocodyliform; integument; sensation; trigeminal; allometry; evolution; brain

Grant sponsors: MU Life Sciences Fellowship; University of Missouri Research Council; the Department of Pathology and Anatomical Sciences.

*Correspondence to: Casey M. Holliday, Integrative Anatomy, Department of Pathology and Anatomical Sciences, University of Missouri, Columbia, MO 65212. E-mail: hollidayca@missouri.edu

Received 24 November 2011; Accepted 14 June 2012.
DOI 10.1002/ar.22666
Published online 13 February 2013 in Wiley Online Library (wileyonlinelibrary.com).

The American alligator (*Alligator mississippiensis*) is one of 23 extant species of crocodylians, a lineage of crocodyliforms that first appeared during the Cretaceous period (Brochu and McEachran, 2000; Brochu, 2003). Alligators are semi-aquatic vertebrates primarily found not only in freshwater areas of the Southeastern United States but also venture into brackish and occasionally saltwater. Alligators have many specialized features for their semi-aquatic lifestyle including a platyrostral skull, a nictitating membrane, a palatal valve that isolates the oral cavity from the choana and pharynx, an external ear flap, elevated eyes, and specialized narial muscles that close the nostrils. In addition to these features alligators, as well as other living crocodylians, have highly sensitive faces packed with receptors that are capable of detecting mechanical stimuli, such as prey or danger, while submerged in water (Soares, 2002).

As in most vertebrates, the fifth cranial nerve, the trigeminal nerve (CN V) detects sensory information from the face of the alligator. This large mixed cranial nerve divides into three major branches: the ophthalmic, maxillary, and mandibular divisions. The ophthalmic and maxillary divisions transmit solely sensory information from the upper face whereas the mandibular division also provides motor innervation to the jaw muscles as well as sensation from the mandible and tongue (Holliday and Witmer, 2007). Beyond somatic touch, several vertebrates evolved trigeminal nerve-based specialized sensory systems such as electroreceptors in the platypus (Gregory et al., 1987; Manger and Perrigrew, 1996) and infrared receptors in some snakes (Molenaar 1974, 1978a,b).

Likewise alligators, and likely all other living crocodylians, are characterized by a group of trigeminal-innervated specialized sensory organs called dome pressure receptors (DPR) (Leitch and Catania, 2012). DPRs are highly sensitive mechanoreceptors which react to changes pressure associated with the movement of water while partially submerged (von During, 1973, 1974; von During and Miller, 1979). Soares (2002) tested the function of DPRs as mechanoreceptors involved in head-orienting behavior by alligators with and without a rubber coating over their faces. Previous research on mechanoreceptor distribution showed that sensitivity is directly proportional to receptor density (Dehnhardt and Kaminski, 1995; Nicolelis et al., 1997). Regions that have mechanoreceptors require additional innervation (Wineski, 1983; Nicolelis et al., 1997; Ebara et al., 2002) and thus the nerve supplying this region, in the case of DPRs, the maxillary and mandibular branches of the trigeminal nerve, will contain more axons, and should be larger as a result.

In crocodylians, the trigeminal nerve roots emerge from the brain at the lateral corner of the medulla oblongata and exit the endocranial cavity through a short passage (the trigeminal foramen) into the trigeminal fossa (Meckel's cave) formed by the laterosphenoid rostrally and prootic caudally (Fig. 1). Here the trigeminal ganglion is seated, surrounded by the laterosphenoid and prootic medially, and the quadrate and pterygoid laterally. Although the ophthalmic nerve exits rostrally from the ganglion through its own trough in the laterosphenoid (Holliday and Witmer, 2009), the maxillary and mandibular branches emerge from the lateral part of the trigeminal ganglion and exit the trigeminal fossa through the maxillomandibular foramen. The maxillary nerve turns rostrally from the maxillomandibular foramen, passing dorsal to m. pterygoideus dorsalis and ventral to the orbit. The mandibular nerve emerges ventrolaterally from the trigeminal ganglion into the adductor chamber, passing between the adductor mandibulae posterior and adductor mandibulae internus, medially, and m. adductor mandibulae externus laterally. During this passage, the nerve gives off several large sensory and motor branches including rami pterygoideus, anguli oris, and caudalis (Holliday and Witmer, 2007). The mandibular nerve passes caudoventrolateral to the cartiliago transiliens, lateral to m. intramandibularis where is gives off the large intermandibular nerve (i.e., mylohyoid nerve), and then passes into the inferior alveolar canal in the mandible just dorsal to Meckel's cartilage. As the mandibular nerve continues through the mandible, it gives off various large and small axons that, along with vasculature, perforate the lateral surface of the dentary. There, the axons terminate in the integument as normal nerve endings, as well as DPRs.

Consequently, numerous neurovascular foramina, forming a "beehive" pattern, rather than the plesiomorphic, lizard-like "linear" pattern (Soares, 2002); characteristically pepper the facial and mandibular elements of crocodylians. Soares (2002) used this pattern of facial foramina as a proxy, or osteological correlate, to infer the evolution of the DPR system in crocodyliforms, reconstructing them as being absent in the Early Jurassic *Protosuchus richardsoni*, a primitive crocodyliform, but also absent in the putative terrestrial Eocene crocodyliform *Sebecus icaeorhinus*. Our own observations of *Sebecus* found, however, that the lateral portion of the symphysis is clearly perforated by numerous neurovascular foramina arranged in a "beehive" pattern, much like that of *Alligator*. Moreover, in tracking the history of the DPR system in crocodyliforms, Soares (2002) only studied a limited number of taxa which were largely sampled from crown-group crocodylians (e.g., *Leidyosuchus canadensis*) or derived neosuchians including *Dyrosaurus phosphaticus*, *Goniopholis sp*., *Pachycheilosuchus trinqui* (formerly the Glen Rose Form), and *Eutretauranosuchus delphi*. Finally, cursory analyses have found little evidence of a clear pattern among DPRs, other sensory nerves, and facial neurovascular foramina (Allen, 2005; Morhardt, 2009; Morhardt et al., 2009) in archosaurs. Thus, the utility of facial neurovascular foramina as osteological correlates of a DPR system remains suspect. On the other hand, larger, more proximal neurovascular foramina, similar to those formed by the larger portions of the crocodylian trigeminal nerves, have proven useful as osteological correlates in testing ecomorphological and evolutionary patterns in the peripheral nervous system. Significant, albeit contentious, correlation was identified between the hypoglossal nerve and the hypoglossal canal in primates, which were used as a proxy for lingual function in speech evolution (Kay et al., 1998; DeGusta, 1999; Jungers et al., 2003). Muchlinski (2008, 2010) showed the primate infraorbital foramen, a presumed proxy for whiskers and facial sensation, correlated with maxillary mechanoreception and potentially foraging ecology.

The presence of the laterosphenoid, which represents the ossified pila antotica, characterizes alligators, crocodyliforms, as well as archosauriforms as a whole

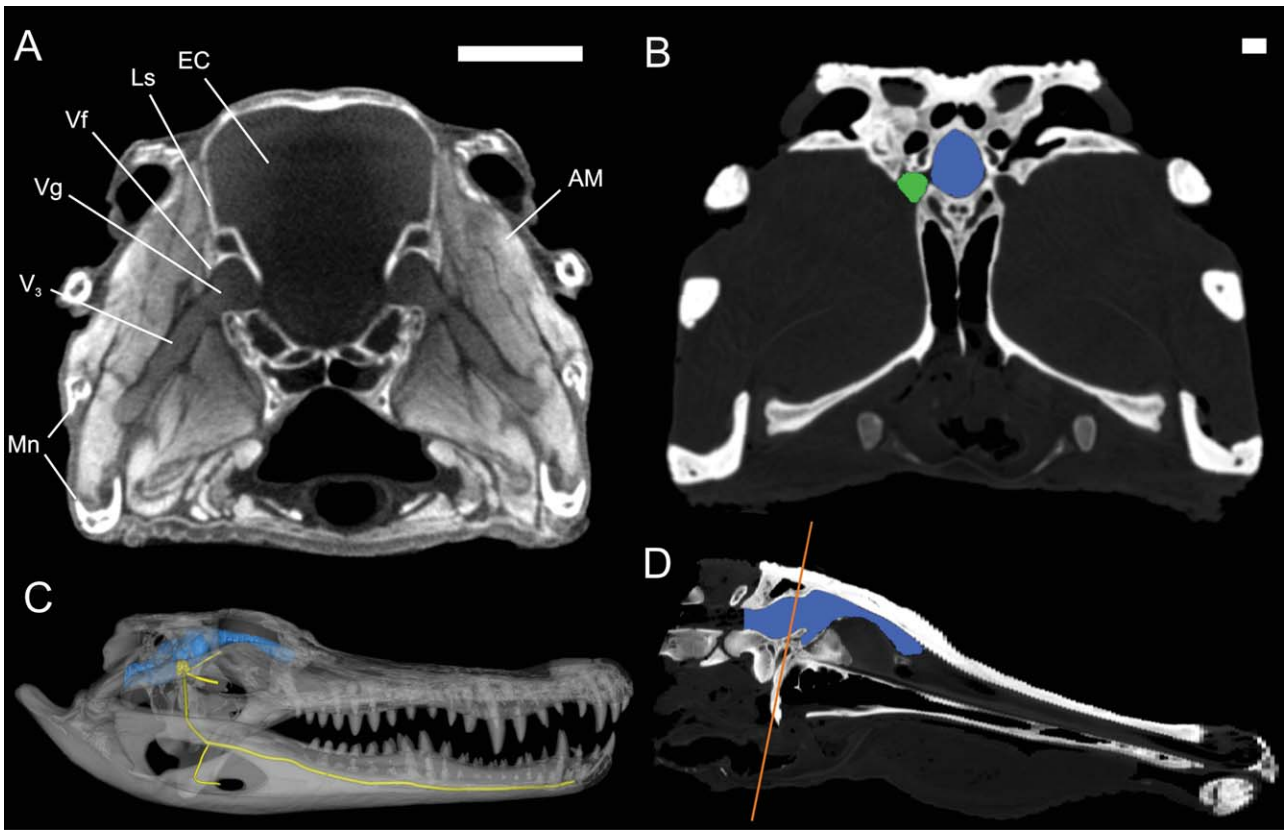

Fig. 1. Imaging and virtual model of alligator specimen. (**A**) Lugol's Iodine enhanced microCT of a juvenile alligator (described in Tsai and Holliday, 2011). (**B**) Axial CT slice from AL005 showing segmentation of the endocast in blue and the trigeminal fossa in green. (**C**) The 3D rendering of the skull (grey) showing the endocast in blue, the trigeminal ganglion in yellow, and the branches of the trigeminal nerve in yellow. (**D**) Sagittal CT slice showing cutting plane from (A) and (B) in orange. Abbreviations: EC, endocranial cavity; Ls, laterosphenoid; Vf, trigeminal fossa; Vg, trigeminal ganglion; V_3, mandibular nerve; Mn, mandible.

(dinosaurs, pterosaurs, and stem taxa). Thus, whereas the trigeminal fossa is only partially ossified in lizards, turtles, and birds, it is surrounded by bone in crocodyliforms and nonavian dinosaurs, making it a faithful "endocast" of the trigeminal ganglion. Therefore, as an archosaur endocranial endocast is generally an accurate proxy for brain size and shape (Hopson, 1979; Witmer and Ridgely, 2009), it is expected that the size of the trigeminal fossa is an accurate representation of the size and shape of the trigeminal ganglion. The bony construction of the trigeminal foramen is quite similar among extant crocodylians (Brochu, 1999) and despite several changes associated with the palate's and epipterygoid's fusion onto the braincase during crocodyliform evolution, the maxillomandibular portion of the foramen has remained largely consistent in its construction over the course of 200 million years of morphological change (Holliday and Witmer, 2009). However, when the DPR system evolved within crocodyliforms, and, if present, how the system was utilized in numerous Mesozoic terrestrial crocodyliform taxa remains unclear.

Thus, insights from the trigeminal nerve may shed new light on the evolution of this important cranial sensory system. Yet, changes in the size of the trigeminal nerve divisions, the trigeminal fossa, and maxillomandibular foramen have not been explored, and the degree, to which these structures scale with the size of the skull and the brain as a whole, is yet unclear. Given that larger nerves and more axons would be necessary to convey the additional sensory fibers necessary for the DPR system, it is expected that the size of the trigeminal fossa, foramen, and related structures would reflect these changes in the innervation patterns of the face. Before inferences can be made about the evolution of the trigeminal system in fossil crocodyliforms, patterns must be tested among extant taxa first.

This article explores the sizes of the trigeminal ganglion, the relative distributions of the mandibular and maxillary nerves, and their relationships to brain and skull size in *Alligator mississippiensis*. We use these metrics to identify scaling relationships among the nervous tissues to gauge the accuracy by which the bony structures reflect the soft tissue anatomy. We then evaluate these results for their implications for sensory distribution along the face of the alligator. Finally, crocodyliforms underwent a significant diversification during the Mesozoic resulting in several independent lineages of marine, semi-aquatic, as well as terrestrial taxa (Brochu, 2003). Thus, it would be expected that changes in the trigeminal system, such as an increase or decrease in relative trigeminal nerve size might accompany life in these varying habitats. Although a

comprehensive evolutionary analysis and transformational hypothesis is beyond the scope of this article, we include relevant metrics from several extant crocodylians including the caiman *Melanosuchus niger* and two crocodylids (*Crocodylus niloticus*, *C. johnstoni* [OUVC 10425]). In addition, we included similarly sized fossil crocodyliform taxa: the semi-aquatic basal brevirostrine *Leidyosuchus canadensis* (ROM 1903); the putatively terrestrial peirosaur *Hamadasuchus rebouli* (ROM 52560); and the marine dyrosaur cf. *Rhabdognathus* (CNRST-SUNY-190) to illustrate the potential utility of trigeminal morphometrics in archosaur and crocodyliform cranial somatosensory evolution.

MATERIALS AND METHODS

Nine frozen heads of *Alligator mississippiensis* were acquired from Rockefeller State Wildlife Refuge (Grand Chenier, LA). Specimen skull lengths, measured from the tip of the snout to the caudal edge of the skull table, ranged from 120.90-mm long to 307.88-mm long representing juvenile (about 120-mm skull length), subadult (ca.190mm), and adult (246–307mm) individuals (Table 1). Body masses were not known. All heads were CT-scanned at Cabell Huntington Hospital, Huntington, WV, or University of Missouri School of Veterinary Medicine at 0.625-mm slice thickness prior to dissection. One large individual (AL025) was imaged with magnetic resonance at the Brain Imaging Center at the University of Missouri, Columbia at a 0.5mm slice thickness using T1 and T2 weighted optimizations. After imaging and dissection, each head was skeletonized (Fig. 2). Additional extant and fossil crocodyliforms were scanned at O'Bleness Memorial Hospital (Athens, OH), Cabell-Huntington Hospital (Huntington, WV) or Royal Veterinary College at 0.625-mm slice thickness.

All CT and MRI data were imported into Amira v5.2 (Visage Imaging) for segmentation and morphometric analysis. The entire skull was segmented from the CT series and the mandibular nerve and proximal maxillary nerve were segmented from the MRI series (Fig. 1). The 3D solid models were generated from the CT segmentation for measurement and analysis. The vertical diameter of the maxillomandibular foramen was measured using both calipers on the macerated skulls and virtual measurement tools on the segmented CT data to test repeatability and similarity of measurement methods. An axial plane traversing the caudal edge of the foramen magnum marked the posterior extent of the endocast. Obliquely parasagittal planes separated each internal cranial foramen from the endocranial cavity. The olfactory tract and bulbs were segmented and included as part of the cranial endocast. The trigeminal fossa was segmented to include all space bounded by the laterosphenoid, prootic, and quadrate. The trigeminal fossa was outlined by a parasagittal plane traversing the trigeminal canal medially, an axial plane through the caudal portion of the ophthalmic canal rostrally, a parasagittal plane traversing the edge of the maxillomandibular foramen laterally, and then the prootic-quadrate suture caudally. The ophthalmic canal was not included in the reconstruction. CT data were segmented in each anatomical plane. Using the CT data, volumes of the endocast and the left trigeminal fossa were segmented and measured.

Histology and Histomorphometry

Specimens were thawed and dissected to expose the left mandibular nerve and left proximal maxillary nerve (Fig. 3). Nerve samples were taken from four sites along the mandibular nerve and one site along the maxillary nerve (Fig. 4). Site V3-1 was the most proximal portion of the mandibular nerve after emerging from the trigeminal ganglion and was sampled to obtain a total count of the axons in the nerve as it emerges from the maxillomandibular foramen with before any branches leave the main nerve. Site V3-2 was immediately distal to the branching of the mylohyoid nerve and was sampled to obtain a count of only sensory axons that pass into the mandible. Site V3-3 was immediately distal to the branching of the internal oral nerve and site V3-4 was

TABLE 1. Skull length, brain, and trigeminal fossa volumes for measured *Alligator mississippiensis* and other crocodyliforms

Specimen	Skull length (sl)	Endocranial volume (ev)	CN V fossa volume (Vfv)	Olfactory tract	Endocranial volume + olfactory tract
AL 001	120.90	3216.65	41.65	353.44	3570.10
AL 002	189.87	7468.46	164.36	1615.88	9084.34
AL 003	127.80	3391.92	58.27	370.65	3762.56
AL 004	189.51	7763.21	161.23	1193.29	8956.49
AL 005	294.37	12720.11	329.76	2982.05	15702.16
AL 015	280.83	10932.13	362.55	2939.42	13871.55
AL 016	307.88	13376.16	337.30	3214.57	16590.73
AL 017	259.28	10550.55	251.18	2009.14	12559.70
AL 025	246.16	9354.26	183.13	1951.10	11305.36
Melanosuchus niger	276.13	20969.65	388.06		
Crocodylus johnstoni	299.10	10723.28	189.14		
Crocodylus niloticus	516.86	30722.77	205.37		
Leidyosuchus. canadensis	380.00	16210.00	430.00		
cf. Rhabdognathus[a]	330.0*	23912.20	151.50		
Hamadasuchus. rebouli	326.90	11527.70	115.30		

Skull length is measured in mm. Brain and trigeminal fossa volumes are measures in mm^3.
[a]*Rhabdognathus* skull length measurement is 274.0 mm but is missing rostralmost portion of snout; we estimated length to be 330.0 mm.

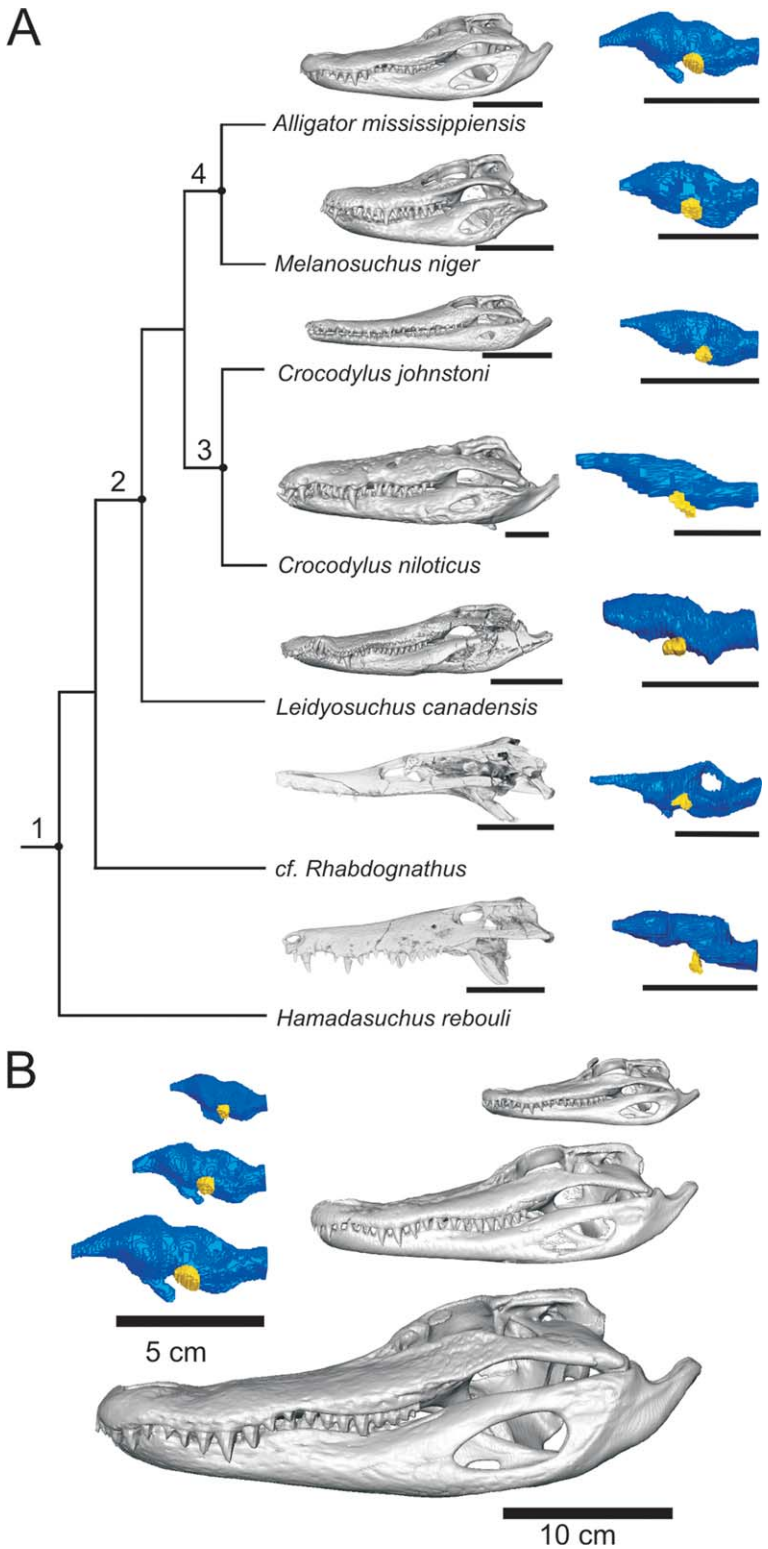

Fig. 2. Anatomy and phylogenetic relationships of extant and fossil crocodyliforms used in this study. (**A**) Left lateral view of skulls and associated endocasts of extant and fossil species included in our study. *Alligator mississippiensis* AL016**,** **Melanosuchus. niger*, **Crocodylus johnstoni* (OUVC 10425), **Crocodylus. niloticus*, *Leidyosuchus canadensis* (ROM 1903), *cf. Rhabdognathus* (CNRST-SUNY-190), *Hamadasuchus rebouli* (ROM 52620). (**B**) Ontogenetic representation from alligator sample with corresponding endocast. *A. mississippiensis* specimens smallest to largest are AL001, AL 04, and AL016. Endocasts are blue and trigeminal ganglion is yellow. Scale bars are ten cm for skulls and five cm for endocasts. Nodes: **1**, Neosuchia; **2**, Crocodylia; **3**, Crocodylidae; **4**, Alligatoridae. *, specimens from personal collection of JR Hutchinson, Royal Veterinary College.

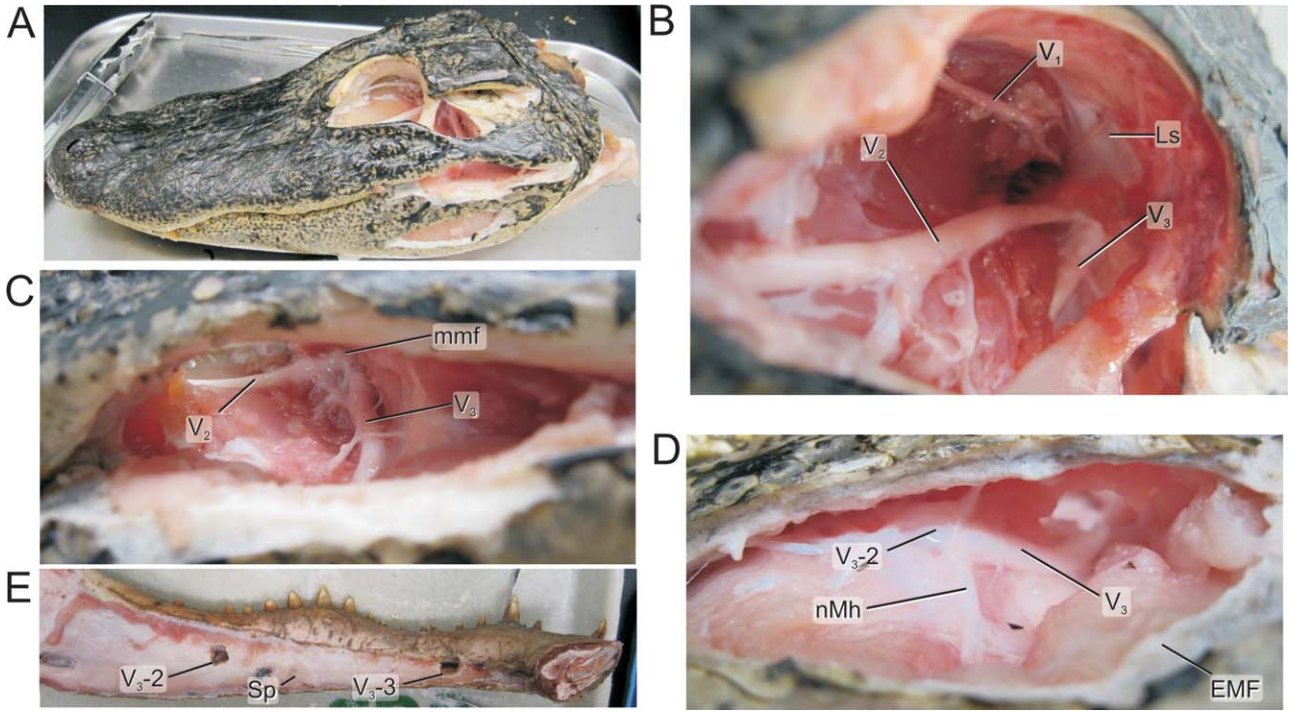

Fig. 3. Soft tissue anatomy of trigeminal nerve (CNV) branches within the alligator head (AL 017). (**A**) Overall dissection of orbit and temporal fossa. (**B**) Dissection of orbit showing the ophthalmic, maxillary, and mandibular divisions of the trigeminal nerve emerging from the lateral wall of the braincase. (**C**) Lateral view of temporal region showing V_2 and V_3 divisions emerging from the maxillomandibular foramen and V_2-5 and V_3-1 sample sites. (**D**) Lateral view of V_3 showing the nerve to mylohyoid branch and V_3-2 sample site. (**E**) Medial view of mandible showing the V_3-3 and V_3-4 sample sites. Abbreviations: V_1, ophthalmic nerve; V_2, maxillary nerve; V_3, mandibular nerve; EMF, external mandibular fenestra; Ls, laterosphenoid; mmf, maxillomandibular foramen; nMh, mylohyoid nerve (intermandibular nerve); Sp, splenial.

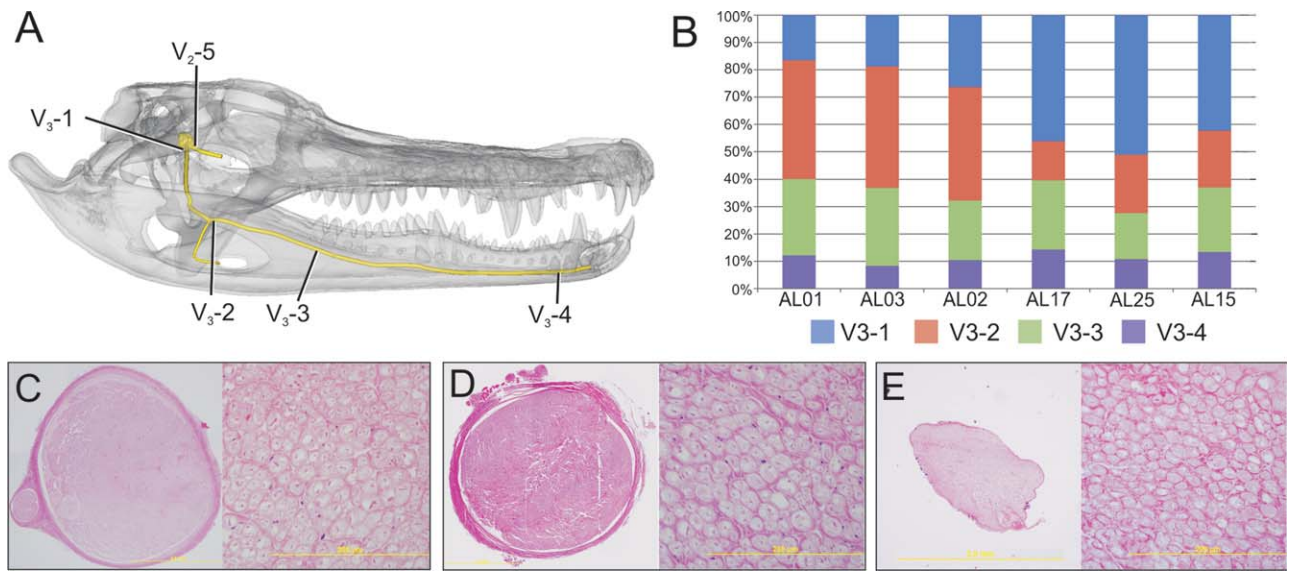

Fig. 4. Nerve histology and relative axon proportions of the trigeminal nerve. (**A**) The 3D model of alligator skull (grey), trigeminal ganglion and trigeminal nerve branches (yellow), and nerve sample sites. (**B**) Proportions of nerve fibers of mandibular nerve at each sample site arranged by skull length. The proximal portion (V_3-1) includes both motor and sensory axons whereas V_3-2 through V_3-4 portions contains only sensory axons. (C-E) Nerve cross sections (V_3-1, V_3-2, and V_3-4 respectively) at ×4 and nerve fibers from each section at ×40.

TABLE 2. Numbers of axons counted at specific sites of trigeminal divisions in *Alligator mississippiensis* as depicted in Fig. 4.

	V3-1			V3-2			V3-3			V3-4			V2-5		
Specimen	Axons	Density	Area	Axons	Density	Area	Axons	Density	Area	Axons	Density	Area	Axons	Density	Area
AL001	26619	478.25	5.065	22232	764	2.648	10661	599.25	1.619	3223	406.67	0.721	16287	574.67	2.579
AL002	26512	282.00	8.574	19531	446.75	3.987	8532	307.00	2.529	2771	227.00	1.111	20425	431.00	4.322
AL003	26162	740.75	3.221	21256	619.75	3.128	9642	647.50	1.358	2165	480.33	0.411	11262	518.75	1.980
AL004	30718	266.50	10.512	14331	253.25	5.161	8842	259.875	3.103	[a]	[a]	[a]	20847	259.875	7.316
AL005	[a]	[a]	[a]	19088	351.00	4.954	14876	359.00	3.775	1208	157.25	0.700	22018	350.25	5.727
AL015	34293	250.50	12.485	29564	264.75	10.184	16292	242.75	6.121	4911	234.50	1.910	17901	253.43	6.442
AL016	31095	226.75	12.507	18400	231.37	7.253	[a]	[a]	[a]	2541	201.67	1.149	13971	148.00	8.609
AL017	37289	299.75	11.333	20106	427.86	4.281	14775	484.00	2.781	5310	462.00	1.047	25895	352.25	6.697
AL025	36228	262.75	12.575	17722	174.00	9.289	10020	200.00	4.569	3868	276.00	1.278	20737	258.75	7.309

Density is equal to the number of axons per ROI as described in Materials and Methods. Area is measured in mm^2.
[a]Nerve site that was unable to be used to obtain an axon count or cross-sectional area.

the most distal portion of the main branch of the mandibular nerve in the mandible that supplies the symphyseal region. Site V2-5 was the most proximal portion of the maxillary nerve and was sampled to provide a comparison to the number of sensory fibers along the upper parts of the face. A Dremel rotary tool was used to expose the inferior alveolar canal and gain access to the distal portions of the mandibular nerve. A section of approximately one cm was excised from each nerve.

Harvested nerves were fixed in 3% glutaraldehyde for 48 hr immediately following dissection. Nerve samples were processed, embedded in paraffin, and sectioned as 5-μm slices on a Leica rotary microtome, mounted, and stained with hematoxylin and eosin (H&E) stain. Nerve slides were photographed on an Olympus BX41TF microscope with an Olympus DP71 at 4× and 40×. Multiple photos of each nerve at 4× magnification were taken and collaged to image the entire nerve cross-section. These images were combined in Adobe Photoshop CS2 and imported into ImageJ to obtain the cross-sectional area of each nerve section. Four 40× images were taken at random sites within each nerve section for individual axon counting. Each of the 40× images was counted manually within ImageJ's Cell Counting module. Total axon number in each nerve cross-section was calculated from the axon number per 40× region of interest and then multiplied by the total cross-sectional area of the nerve to estimate the total number of axons in each cross-section. Scaling relationships among variables were determined via reduced major axis (RMA) regression analysis conducted in NCSS 2007 statistical software using an adjusted R (Rbar) for small sample size, R-squared, a post hoc Bonferroni adjusted *P* value, and slope analysis using confidence intervals to test the hypothesis that the experimentally derived slope differed from that expected for particular equations for isometry.

RESULTS

Axon Count

After sectioning and mounting all nerve samples, three sites out of 45 were of unsuitable quality for cross-sectional area or axon counting. It was noted that axon density was uniform across the sample except for the two youngest specimens. The sub adult and adult nerves had an average density of 285 axons per ROI (±70). The juvenile nerves had an average density of 583 axons per ROI (±26).

Mean axon count was 31,115 (±4,480 SD) at site V3-1; 20,248 (±4,160) at site V3-2; 11,705 (±3,093) at site V3-3; 3,249 (±1,387) at site V3-4; and 18,815 (±4,452) at site V2-5. Mean cross-sectional area was 9.5 mm^2 (±3.6 mm^2) at site V3-1; 5.6 mm^2 (±2.7 mm^2) at site V3-2; 3.3 mm^2 (±1.6 mm^2) at site V3-3; 1.1 mm^2 (±0.5 mm^2) at site V3-4; and 5.66 mm^2 (2.25 mm^2) at site V2-5. Full nerve cross-sectional area and axon count for each sample site are recorded in Table 2.

In the six specimens that had all four sites along the mandibular nerve well represented, about 28.59% of the total number of axons branched away from the main trunk before site V3-2. These fibers include virtually all of the motor rami to the jaw muscles as well as several significant sensory rami. Another 32.71% of the total number of axons branched between V3-2 and V3-3. This means that about 40% of the mandibular nerve solely innervates the mandible proper. Within the mandible, 26.46% of the total number of axons branched between V3-3 and V3-4 and 12.24% of the total number of axons terminated after site V3-4.

Endocast and Trigeminal Fossa Volume

Mean endocast volume for the sample was 8,753 mm^3 (±3,665 mm^3). Further separating the sample into juvenile, subadult, and adult ages we find endocranial volume averages of 3304 mm^3 (±124 mm^3), 7,616 mm^3 (±208 mm^3), and 11,387 mm^3 (±1,641 mm^3), respectively. Mean trigeminal fossa volume for the sample was 210 mm^3 (±118 mm^3). Separation by approximate aged yielded 50 mm^3 trigeminal fossa volume (±12 mm^3) for juvenile, 163 mm^3 (±2 mm^3) for subadult, and 293 mm^3 (±74 mm^3) for adult alligators. Full results for volumes are shown in Table 1.

Scaling Analysis

The volume of the trigeminal fossa correlated significantly with endocranial volume ($r = 0.98$) and skull length ($r = 0.98$) (Table 3, Fig. 5). Endocast volume correlated significantly with skull length ($r = 0.99$). The vertical diameter of the maxillomandibular foramen strongly correlates with the volume of the trigeminal fossa ($r = 0.93$). The maxillomandibular foramen

TABLE 3. Results of regression analysis of skeletal variables including variables (*y* vs. *x*), regression equation, adjusted Pearson correlation coefficient (*r*), R^2, *P* value, expected slope of isometry, and confidence interval of regression slope (CI)

Variables (*y* v *x*)	Equation	*r*	R^2	*P* value	Isometry	CI
Alligator						
Log mmf × log sl	$y = (-0.5686) + (0.6102)x$	0.96	0.90	0.0001	1.0	0.44–0.78
Log ev × log sl	$y = (0.4246) + (1.4909)x$	0.99	0.97	0.0001	3.0	1.27–1.71
Log Vfv × log sl	$y = (-2.7741) + (2.1494x$	0.98	0.95	0.0001	3.0	1.73–2.57
Log mmf × log ev	$y = (-0.7298) + (0.4060)x$	0.96	0.91	0.0001	0.33	0.30–0.51
Log Vfv × log ev	$y = (-3.3506) + (1.4326)x$	0.98	0.96	0.0001	1.0	1.20–1.67
Log mmf × log Vfv	$y = (0.2465) + (0.2715)x$	0.93	0.86	0.0002	0.33	0.18–0.36
Log V3.1 axon count × log sl	$y = (0.2854) + (3.8249)x$	0.74	0.49	NS	1.0	0.06–0.52
Log V2.5 axon count × log sl	$y = (0.3318) + (3.4901)x$	0.46	0.09	NS	1.0	−0.25–0.91
Log mmf axon count × log sl	$y = (0.301) + (3.9928)x$	0.67	0.37	NS	1.0	0.01–0.60
Log V3.1 axon count × log mmf	$y = (0.4149) + (4.136)x$	0.89	0.74	0.0018	1.0	0.03–0.80
Log V2.5 axon count × log mmf	$y = (0.5745) + (3.7731)x$	0.91	0.79	0.0008	1.0	0.31–1.45
Log mmf axon count × log mmf	$y = (0.4695) + (4.2936)x$	0.67	0.37	NS	1.0	0.01–0.94
Pooled *Alligator* (AL015) and six additional crocodyliforms						
Log mmf × log sl	$y = (0.7395) + (5.0727)x$	0.06	0.03	NS		
Log ev × log sl	$y = (1.1629) + (1.2089)x$	0.62	0.27	NS		
Log Vfv × log sl	$y = (3.3214) + (-0.3752)x$	0.16	0.17	NS		
Log Vfv × log ev	$y = (2.2418) + (3.1176)x$	0.03	0.20	NS		
Log mmf × log ev	$y = (-0.1239) + (0.2351)x$	0.50	0.10	NS		
Log mmf × log Vfv	$y = (0.2336) + (0.2672)x$	0.70	0.39	NS		

Bonferroni adjusted *P* for Alligator-only data is $P = 0.0042$; for pooled data is $P = 0.0083$. NS, not significant. Abbreviations: ev, endocast volume; mmf, maxillomandibular foramen diameter; sl, skull length; Vfv, trigeminal fossa volume.

significantly correlates with skull length ($r = 0.96$) and endocast volume ($r = 0.96$).

The number of axons and nerve cross sectional area at each sample site show positive allometry with skull length and trigeminal fossa volume except for at site V3-2. At V3-2, the number of axons correlates with skull size and trigeminal fossa volume but scales with negative allometry. Axon density at each sample site also shows a pattern of significant correlation and negative allometry with skull length and trigeminal fossa volume.

DISCUSSION

The results illustrated here indicate that head length, brain size, and trigeminal nerve size are consistently related to each other in *Alligator mississippiensis*. Despite the small sample size, the distribution of axons is largely uniform across all individuals. The larger, adult individuals appear to have more nerves branching within the adductor chamber (i.e., between sites V3-1 and V3-2) compared to smaller individuals (Figs. 2 and 4). However, it remains unclear to what degree these changes are due to increases in motor or sensory function. The decrease in axon density as individuals grow older is most likely due to the additional space occupied by the myelin sheath around each axon. Axon diameter as well as the conduction velocity of peripheral nerves relates to the thickness of the myelin sheath (Kiernan et al., 1996; Kandel et al., 2000; Michailov et al., 2004; Moldovan et al., 2006). Although the thickness of the myelin sheath does not continue to grow throughout ontogeny, the youngest alligators sampled in our study may not have completed myelination of their axons.

The sizes of the maxillary and mandibular nerves relate to the magnitude of sensory coverage as well as different sensory modalities that are carried by these nerves. Because densely packed mechanoreceptors affect the size of a nerve (Muchlinski, 2010), their presence, as well as absence, in a somatic region is reflected in axon count and nerve fiber size. These results show axon count and nerve cross-sectional area correlates with both trigeminal fossa volume and skull length in *Alligator*. Assuming that other extant crocodylians follow the same pattern, the trigeminal fossa volume and diameter of the maxillomandibular foramen are informative metrics for inferring trigeminal nerve size, and therefore informative proxies for facial sensitivity, mechanoreception, and other sensory input.

Comparative Utility in Fossils

These results indicate that foramen size may be an accurate predictor of nerve size and axon number in fossil crocodyliforms. These findings are also important for inferring sensory receptor density in soft tissue from only skeletal sources. Previous investigations on cranial nerves and their branches with respect to foramen size (DeGusta, 1999; Muchlinski, 2008) and sensory mechanoreceptors (Soares, 2002; Muchlinski, 2010) agree with our results. More sensory receptors innervated by the maxillary and mandibular nerves will require more axons within each nerve (Kandel et al., 2000), thus larger nerves, and a larger trigeminal ganglion size.

To illustrate the use of the *Alligator* data in a small case study, we collected relevant data from: three extant crocodyliform species, *Crocodylus niloticus*, *Crocodylus johnstoni*, and *Melanosuchus niger*; and three extinct crocodyliforms, the basal eusuchian *Leidyosuchus canadensis*, the sebecid neosuchian *Hamadasuchus rebouli*, and the dyrosaurid neosuchian *cf. Rhabdognathus* (Fig. 2). These fossil taxa have similar skull lengths and occupied different ecological niches. *Leidyosuchus canadensis*

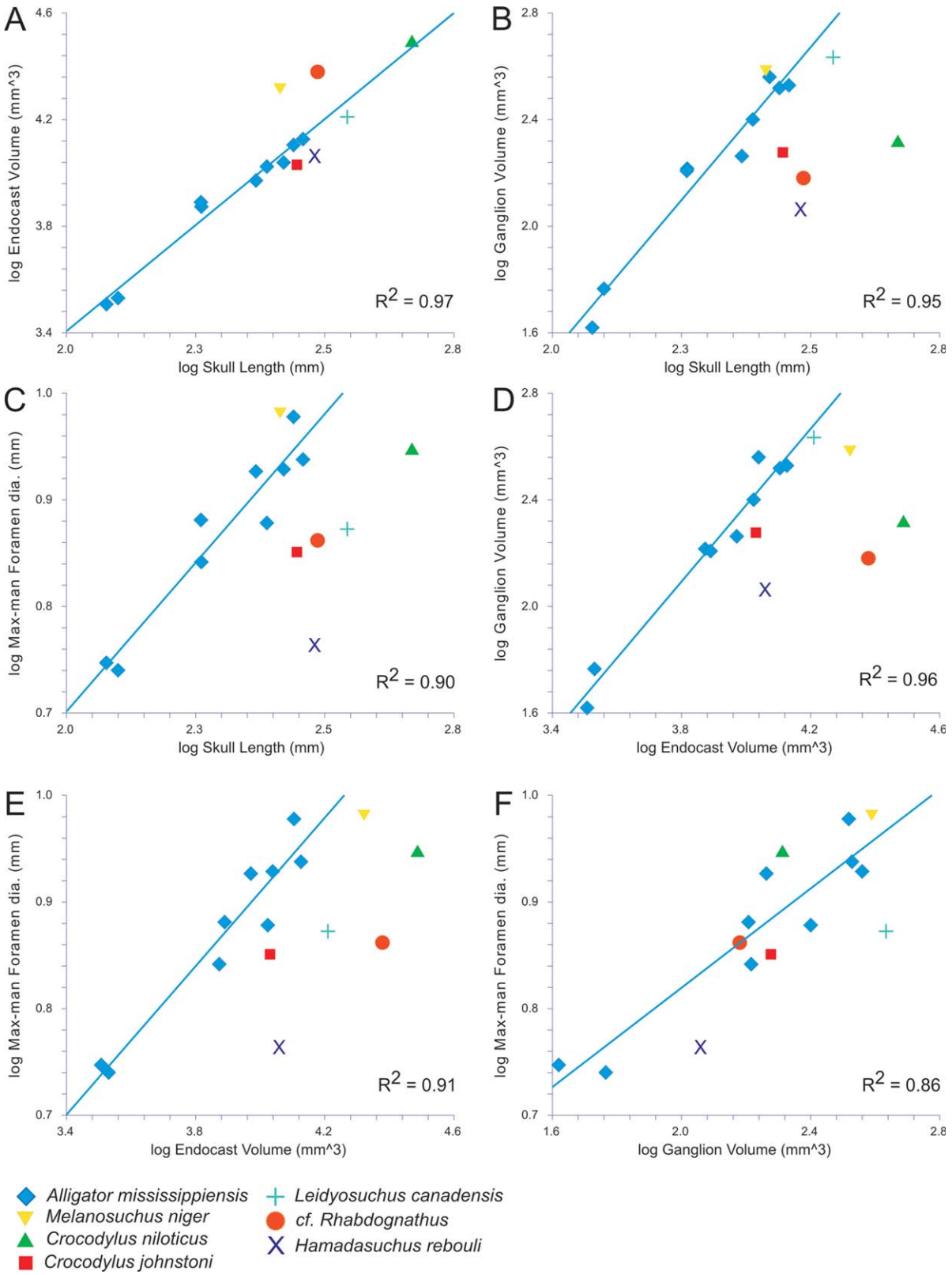

Fig. 5. Scaling analysis of alligators with supplemental extant and fossil crocodyliforms. (**A–F**) Blue line is the regression of *Alligator*-only sample with R^2 as reported in Table 3. Additional extant and fossil crocodyliforms identified in Key.

(ROM 1903) is a basal brevirostrine crocodylian, an early representative of the clade containing crocodiles, alligators and caimans (Brochu and McEachran, 2000; Brochu, 2003), from Late Cretaceous of North America. It bears numerous features similar to modern alligators including a platyrostral, triangular skull, mediolaterally broad occiput, and a dense array of facial neurovascular foramina (Soares, 2002). *Rhabdognathus* (CNRST-SUNY-190; Brochu et al., 2002) is a short-snouted dyrosaur from the Paleocene of Northern Africa. Dyrosaurs were marine neosuchian crocodyliforms characterized by very long, slender snouts, enlarged dorsotemporal fossae, rectangular occiputs, and some facial neurovascular pitting. *Hamadasuchus rebouli* (ROM 52620) has a tall, oreinirostral skull with some facial neurovascular pitting, and is a terrestrial predator related to sebecid neosuchian crocodyliforms (Larsson and Sues, 2007). Like the *Alligator* sample, each specimen was CT-scanned at 0.625-mm slice thickness, had its cranial and trigeminal endocasts reconstructed and other measurements collected.

No significant correlations were found among fossil and extant species data pooled with an alligator of similar skull length (AL015). The relationships between cranial endocast volume and skull length ($r = 0.62$) and maxillomandibular foramen diameter and trigeminal fossa volume ($r = 0.70$) are strong. However, the relationships between trigeminal fossa volume and skull length ($r = 0.16$), and cranial endocast volume ($r = 0.03$) are weak. These findings suggest that differences in trigeminal fossa volume relative to brain or skull size may be due to differences in sensory magnitude rather than relative differences with nervous tissue as a whole (Table 3, Fig. 5). Although a larger sample size is necessary to understand the relationships between the skull, brain, and trigeminal nerve in crocodyliforms, we interpret the lack of clear signal among these variables to be result of phylogenetic or behavioral effects associated with adaptations of the cranial sensory system rather than size alone.

Leidyosuchus had endocranial and trigeminal fossa volumes similar to an alligator of similar skull length. *Rhabdognathus* had a large endocranial volume compared to that expected for an alligator of similar skull length and a trigeminal fossa volume that is similar to that found in a similar-sized alligator. *Hamadasuchus* had small endocranial and trigeminal fossa volumes compared to an alligator of similar size and a relatively small trigeminal fossa in relation to its endocranial volume. Thus, *Hamadasuchus* and *Rhabdognathus* had smaller trigeminal fossae, and thus likely decreased facial sensation compared to *Leidyosuchus* and *Alligator*. Several hypotheses could explain this pattern, though they remain poorly supported given our small sample size. First, the larger trigeminal ganglia found in *Leidyosuchus* and *Alligator* may be derived compared to other crocodyliforms and reflect eusuchian origins of the derived DPR system. Second, the smaller trigeminal ganglia in *Hamadasuchus* and *Rhabdognathus* may reflect an ecologically relevant, diminished sense of face touch compared to other crocodyliforms. One might expect that terrestrial crocodyliforms such as *Hamadasuchus* had less need for DPR-based facial sensation, and thus possessed smaller trigeminal ganglia. However, the decreased ganglion size in the marine dyrosaur supports the hypothesis that the DPR system was an emergent system among early eusuchians and not a primitive feature of neosuchian crocodyliforms. However, it is equally possible that dyrosaurs secondarily lost an enhanced DPR system for reasons still unclear. Regardless, this study demonstrates that trigeminal ganglion size is an informative metric for analyzing sensory adaptations in crocodyliforms and potentially other fossil archosaurs. Further investigation into the rich crocodyliform fossil record may elucidate how different taxa responded to environmental cues and when the neurologic osteological correlates of the DPR system first appeared.

Our investigation of the alligator trigeminal fossa and peripheral branches of the trigeminal nerve shows a relationship between trigeminal fossa size, and thus trigeminal ganglion, and skull length. These findings support the idea that crocodyliforms of a given head size, should have a predictable sensory sensitivity based on skeletal data. With the future addition of other species to such investigations, it will be possible to make better inferences about the sensory potential in species where only fossil data are available. More in-depth analysis of alligator soft tissues, specifically the most terminal branches of the trigeminal nerves as well as DPRs will help infer not only the sensory spread in an extinct species, but also which sensory modalities may have been present. With application of similar anatomical data on extant species as a baseline, these findings suggest that neurologic osteological correlates of the trigeminal system are informative features useful for investigating crocodyliform as well as archosaur somatosensory evolution.

ACKNOWLEDGEMENTS

The authors thank undergraduates J. Kim, R.J. Skiljan, and C. Gant for assistance in the lab. They thank Ruth Elsey and Rockefeller State Refuge, LA for supplying alligator material. They thank JR Hutchinson (Royal Veterinary College), La Ferme Aux Crocodiles, France and St. Augustine Alligator Farm, US for sharing data of *C. niloticus* and *M. niger* and LM Witmer (Ohio University) for sharing CT data of *cf. Rhabdognathus* and *C. johnstoni* (via JRH).

LITERATURE CITED

Allen D. 2005. The inferred evolutionary history of integumentary sense organs in crocodylomorphs. J Vertebr Paleontol 25(Suppl to 3):31A.

Brochu CA. 1999. Phylogenetics, taxonomy, and historical biogeography of Alligatoroidea. J Vertebr Paleontol 19:9–100.

Brochu CA. 2003. Phylogenetic approaches toward crocodylian history. Annu Rev Earth Pl Sci 31:357–397.

Brochu CA, McEachran JD. 2000. Phylogenetic relationships and divergence timing of *Crocodylus* based on morphology and the fossil record. Copeia 2000:657–673.

Brochu CA, Bouaré ML, Sissoko F, Roberts EM, O'Leary MA. 2002. A dyrosaurid crocodyliform braincase from Mali. J Paleontol 76:1060–1071.

DeGusta D, Gilbert W, Turner S. 1999. Hypoglossal canal size and hominid speech. Proc Natl Acad Sci USA 96:1800–1804.

Dehnhardt G, Kaminski A. 1995. Sensitivity of the mystacial vibrissae of harbor seals (*Phoca vitulina*) for size differences of actively touched objects. J Exp Biol 198:2317–2323.

Ebara S, Kumamoto K, Matsuura T, Mazurkiewicz J, Rice F. 2002. Similarities and differences in the innervation of mystacial vibrissal follicle-sinus complexes in the rat and cat: a confocal microscopic study. J Comp Neurol 449:103–119.

Gregory JE, Iggo A, Mcintyre AK, Proske U. 1987. Electroreceptors in the platypus. Nature 326:386–387.

Holliday CM, Witmer LM. 2007. Archosaur adductor chamber evolution: integration of musculoskeletal and topological criteria in jaw muscle homology. J Morphol 268:457–484.

Holliday CM, Witmer LM. 2009. The epipterygoid of crocodyliforms and its significance for the evolution of the orbitotemporal region of eusuchians. J Vertebr Paleontol 29:715–733.

Hopson JA. 1979. Paleoneurology; pp. 39–146 *in* C. Gans (ed.), Biology of the Reptilia Academic Press, New York.

Jungers WL, Pokempner AA, Kay RF, Cartmill M. 2003. Hypoglossal canal size in living hominoids and the evolution of human speech. Hum Biol 75:473–484.

Kandel E, Schwartz J, Jessell T. 2000. Principals of neural science. 4th ed. New York: McGraw-Hill.

Kay RF, Cartmill M, Balow M. 1998. The hypoglossal canal and the origin of human vocal behavior. Proc Natl Acad Sci USA 95:5417–5419.

Larsson HCE, Sues H-D, 2007. Cranial osteology and phylogenetic relationships of *Hamadasuchus rebouli* (Crocodyliformes: Mesoeucrocodylia) from the Cretaceous of Morocco. Zool J Linn Soc 149:533–567.

Leitch DB, Catania KC. 2012. Structure, innervation and response properties of integumentary sensory organs in crocodilians. Journal of Experimental Biology 215:4217–4230.

Kiernan MC, Mogyoros I, Burke D. 1996. Differences in the recovery of excitability in sensory and motor axons of human median nerve. Brain 119:1099–1105.

Manger PR, Perrigrew JD. 1996. Ultrastructure, number, distribution and innervation of electroreceptors and mechanoreceptors in the bill skin of the platypus, *Ornithorhynchus anatinus* (part 1 of 2). Brain Behav Evol 48:27–40.

Michailov GV, Sereda MW, Brinkmann BG, Fischer TM, Haug B, Birchmeier C, Role L, Lai C, Schwab MH, Nave K. 2004. Axonal neuregulin-1 regulates myelin sheath thickness. Science 304:700–703.

Moldovan M, Sorensen J, Krarup C. 2006. Comparison of the fastest regenerating motor and sensory myelinated axons in the same peripheral nerve. Brain 129:2471–2483.

Molenaar GJ. 1974. An addition trigeminal system in certain snakes possessing infrared receptors. Brain Res 78:340–344.

Molenaar GJ. 1978a. The sensory trigeminal system of a snake in the possession of infrared receptors. I. The sensory trigeminal nuclei. J Comp Neurol 179:123–135.

Molenaar GJ. 1978b. The sensory trigeminal system of a snake in the possession of infrared receptors. II. The central projections of the trigeminal nerve. J Comp Neurol 179:137–151.

Morhardt A. 2009. Dinosaur smiles: do the texture and morphology of the premaxilla, maxilla, and dentary bones of sauropsids provide osteological correlates for inferring extra-oral structures reliably in dinosaurs? MS Thesis, Western Illinois State University, Macomb, IL.

Morhardt A, Bonnan MF, Keiler T. 2009. Dinosaur smiles: correlating premaxilla, maxilla, and dentary foramina counts with extra-oral structures in amniotes and its implications for dinosaurs. J Vert Paleont, 29 (Suppl to 3): 152A.

Muchlinski MN. 2008. The relationship between the infraorbital foramen, infraorbital nerve, and maxillary mechanoreception: implications for interpreting the paleoecology of fossil mammals based on infraorbital foramen size. Anat Rec 291:1221–1226.

Muchlinski MN. 2010. A comparative analysis of vibrissa count and infraorbital foramen area in primates and other mammals. J Hum Evol 58:447–473.

Nicolelis M, Lin R, Chapin J. 1997. Neonatal whisker removal reduces the discrimination of tactile stimuli by thalamic ensembles in adult rats. J Neurophysiol 78:1691–1706.

Soares D. 2002. An ancient sensory organ in crocodilians. Nature 417:241–242.

Tsai HP, Holliday CM. 2011. Ontogeny of the alligator cartilage transiliens and its significance for sauropsid jaw muscle evolution. PLoS One 6:e24935.

von During M. 1973. The ultrastructure of lamellated mechanoreceptors in the skin of reptiles. Anat Embryol 143:81–94.

von During M. 1974. The ultrastructure of the cutaneous receptors in the skin of *Caiman crocodilus*. Abhandlungen Rhein.-Westfal. Akad 53:123–134.

von During M, Miller MR. 1979. Sensory nerve endings in the skin and deeper structures. In: Gans C, Northcutt RG, Ulinski P, editors. Biology of the reptilia, 9. Neurology A. New York: Academic Press. p 407–442.

Wineski L. 1983. Movement of the cranial vibrissae in the golden hamster (*Mesocritus auratus*). J Zool 200:261–280.

Witmer LM, Ridgely RC. 2009. New insights into the brain, braincase, and ear region of tyrannosaurs (Dinosauria, Theropoda), with implications for sensory organization and behavior. Anat Rec 292:1266–1296.